NIH Public Access
Author Manuscript
J Biomed Opt. Author manuscript; available in PMC 2009 November 30.

Published in final edited form as:
J Biomed Opt. 2006 ; 11(2): 021002. doi:10.1117/1.2192697.

Optical coherence tomography for imaging the vulnerable plaque

Guillermo J. Tearney,
Wellman Center for Photomedicine, Department of Pathology, Massachusetts General Hospital, 50 Blossom Street, BAR703, Boston, Massachusetts 02114

Ik-Kyung Jang, and
Massachusetts General Hospital, Cardiology Division, 55 Fruit Street, BAR703, Boston, Massachusetts 02114

Brett E. Bouma
Wellman Center for Photomedicine, Massachusetts General Hospital, 50 Blossom Street, BAR703, Boston, Massachusetts 02114

Abstract

While our understanding of vulnerable coronary plaque is still at an early stage, the concept that certain types of plaques predispose patients to developing an acute myocardial infarction continues to be at the forefront of cardiology research. Intracoronary optical coherence tomography (OCT) has been developed to both identify and study these lesions due to its distinct resolution advantage over other imaging modalities. We review clinical research conducted at the Massachusetts General Hospital over the past five years to develop, validate, and utilize this technology to improve our understanding of vulnerable plaque. Our results show that intracoronary OCT may be safely conducted in patients and that it provides abundant information regarding plaque microscopic morphology, which is essential to the identification and study of high-risk lesions. Even though many basic biological, clinical, and technological challenges must be addressed prior to widespread use of this technology, the unique capabilities of OCT ensure that it will have a prominent role in shaping the future of cardiology.

Keywords

medical imaging; coherence

1 Introduction

Acute myocardial infarction (AMI) is a leading cause of death in the United States and industrialized countries.[1,2] Research conducted over the past 15 years has demonstrated that several types of minimally or modestly stenotic atherosclerotic plaques, termed vulnerable plaques, are precursors to coronary thrombosis, myocardial ischemia, and sudden cardiac death. Postmortem studies have identified one type of vulnerable plaque, the thin-cap fibroatheroma (TCFA), as the culprit lesion in approximately 80% of sudden cardiac deaths.[3–7] Over 90% of TCFAs are found within the most proximal 5.0 cm segment of each of the main coronary arteries [left anterior descending (LAD); left circumflex (LCx); and right coronary artery (RCA)].[3,5] The TCFA is typically a minimally occlusive plaque characterized

© 2006 Society of Photo-Optical Instrumentation Engineers.

Address all correspondence to Guillermo J. Tearney, Wellman Center for Photomedicine, Massachusetts General Hospital, Boston, MA 02114. Tel: 617–724–2979; Fax: 617–726–4103; gtearney@partners.org.

NIH-PA Author Manuscript
NIH-PA Author Manuscript
NIH-PA Author Manuscript

NIH-PA Author Manuscript

NIH-PA Author Manuscript

NIH-PA Author Manuscript

histologically by the following features: (1) thin fibrous cap (<65 μm), (2) large lipid pool, and (3) activated macrophages near or within the fibrous cap.[3,5,7–9] It is hypothesized that these features predispose TCFAs to rupture in response to biomechanical stresses.[10,11] Following rupture and the release of procoagulant proteins, such as tissue factor, a substrate for thrombus formation is created, leading to an acute coronary event.[12,13] While TCFAs are associated with the majority of AMIs, recent autopsy studies have shown that coronary plaques with erosions or superficial calcified nodules may also precipitate thrombosis and sudden occlusion of a coronary artery.[3,5,14,15]

Although autopsy studies have been valuable in determining features of culprit plaques, the retrospective nature of these studies limits their ability to quantify the risk of an individual plaque for causing acute coronary thrombosis. For instance, TCFAs are a frequent autopsy finding in asymptomatic or stable patients and are found with equal frequency in culprit and nonculprit arteries in acute coronary syndromes.[16] Moreover, disrupted TCFAs have been found in 10% of non-cardiac deaths.[16] Recent findings of multiple ruptured plaques[17] and increased systemic inflammation in acute patients[18–20] has challenged the notion of a single vulnerable plaque as the precursor for AMI.[19,21,22] An improved understanding of the natural history and clinical significance of these lesions would accelerate progress in diagnosis, treatment, and prevention of coronary artery disease (CAD).

An attractive approach to studying the evolution of vulnerable plaques is noninvasive or intracoronary imaging of individual lesions at multiple time points. Unfortunately, the microscopic features that characterize vulnerable plaque are not reliably identified by conventional imaging technologies such as intravascular ultrasound (IVUS),[23–28] CT,[29–32] and MRI.[32–35] While experimental intracoronary imaging modalities such as integrated backscatter IVUS,[36,37] elastography,[32,38] angioscopy,[39–43] near-infrared spectroscopy,[44] fluorescence spectroscopy,[45–47] Raman spectroscopy,[48,49] and thermography[50,51] have been investigated for the detection of vulnerable plaque, no method to date has been shown to reliably identify all of the characteristic features of these lesions.

2 Optical Coherence Tomography

Intracoronary optical coherence tomography (OCT) is an invasive microscopic imaging technology that has been developed for the identification of vulnerable plaque.[52–55] OCT acquires cross-sectional images of tissue reflectance and, since it may be implemented through an optical fiber probe, it is readily adaptable to coronary catheters[56] for insertion into coronary arteries and circumferential imaging of arterial pathology. The first investigation of vascular optical coherence tomography ex vivo demonstrated the potential of this technique to identify arterial microstructure.[57] Subsequent development of OCT technology enabled image acquisition at rates sufficient for intracoronary imaging in human patients.[58–60] In this manuscript, we review studies conducted with this technology over the past five years at the Massachusetts General Hospital (MGH). Results from these studies show that a wide variety of microscopic features, including those associated with TCFAs, can be identified by OCT imaging both ex vivo and in living human patients. These findings suggest that this technology will play an important role in improving our understanding of coronary artery disease, guiding local therapy, and decreasing the mortality of AMI.

3 Optical Coherence Tomography System

A schematic of the OCT system is shown in Fig. 1.[59] Briefly, the system consists of a polarization-diverse fiber-optic non-reciprocal interferometer, which operates in the time domain. The light source is centered at 1300 nm and has a Gaussian spectral full-width-at-half-maximum of 70 nm, providing an axial resolution of approximately 8 μm in tissue. The transverse resolution, determined by the focal spot size produced by the probe, is 25 μm. Group

NIH-PA Author Manuscript

NIH-PA Author Manuscript

NIH-PA Author Manuscript

delay scanning at a rate of 2 kHz was conducted by utilizing a phase-control rapidly scanning optical delay (RSOD) in the reference arm.[61] Images (500 pixels transverse × 250 pixels axial) were obtained at 4 frames/ s and stored digitally. A custom-built fiber-optic rotary junction was utilized for catheter-based circumferential imaging and a galvanometer mirror was used for the free-space experiments.[62] Catheters were constructed by modifying a commercially available 3.0 F (950 μm diameter), rapid-exchange IVUS catheter to incorporate a central fiber, a distal gradient index (GRIN) lens, and a deflecting prism, which were rotated to construct a circumferential image.[62]

4 Ex Vivo Studies

4.1 Plaque Characterization

The first steps in validating this imaging modality were to establish and test the accuracy of objective image criteria for discrimination of atherosclerotic plaque types ex vivo. A total of 357 specimens (162 aortas, 105 carotid bulbs, and 90 coronary arteries) were obtained from 90 cadavers (48 male, 42 female, mean age 74.5±13.25). The specimens were imaged fresh at 37°C, less than 72 h postmortem. Registration was accomplished by placing ink marks on the tissue prior to imaging so that both OCT images and histopathology slides contained visibly recognizable reference points. Following imaging, specimens were fixed in Formalin and processed for paraffin embedding, 5-μm sectioning, and staining (H&E, Trichrome, Movat's Pentachrome, and immunohistochemistry). For the training set, 50 cadaver plaques were imaged by OCT and correlated with histology obtained at the imaging site.[55] Fibrous plaques were characterized by homogeneous, signal-rich regions, fibrocalcific plaques by signal-poor regions with sharp borders, and lipid-rich plaques by signal-poor regions with diffuse borders (Fig. 2). Two blinded readers prospectively applied these criteria to images of the remaining 307 plaques (validation set). Using histopathologic diagnosis as the gold standard, the accuracy of OCT for characterizing plaque type was then determined. These criteria yielded a sensitivity and specificity ranging from 71–79% and 97–98%, for fibrous plaques, 95–96% and 97% for fibrocalcific plaques, and 90–94% and 90–92% for lipid-rich plaques, respectively (overall agreement, $\kappa = 0.84$).[55] These results demonstrated that objective OCT criteria are highly sensitive and specific for differentiating lipid-rich plaques from other plaque types.[55]

4.2 Quantification of Macrophage Content

Macrophages are central to the etiology of coronary artery disease.[12,63–65] Due to the high quantity of intracellular phagolysosomes containing lipid and other cellular debris, we hypothesized that the refractive index contrast provided by the cytoplasm of macrophages would result in a strong optical signal from these cells (Fig. 3). Furthermore, since macrophages are typically heterogeneously distributed in atherosclerotic tissue, the spatial variance of OCT signal in plaques with high macrophage content should also be elevated. In order to test this hypothesis, cap macrophage and smooth muscle densities of 27 necrotic core fibroatheromas were quantified by analyzing indirect horseradish immunoperoxidase staining of paraffin embedded tissue sections incubated with CD68 and smooth muscle actin monoclonal antibodies, respectively.[66] Hematoxylin was the counter-stain. Morphometric measurements (single 10× cross-sectional field) of cell density (% area stained) within a 500-μm (lateral) × 125-μm (axial) region of interest were then compared to the normalized standard deviation (NSD) of the OCT signal intensity at corresponding locations.[66] We found a high degree of positive correlation between OCT and histologic measurements of fibrous cap macrophage density ($r=0.84$, $p<0.0001$) and a negative correlation between OCT and histologic measurements of smooth muscle actin density ($r=-0.56$, $p<0.005$). A range of NSD thresholds (6.15–6.35%) yielded greater than 90% sensitivity and specificity for identifying caps containing >10% CD68 staining. This study demonstrated that the high contrast and resolution

NIH-PA Author Manuscript

NIH-PA Author Manuscript

NIH-PA Author Manuscript

of OCT enables the quantification of macrophages within fibrous caps of atherosclerotic plaques.

4.3 Other Plaque Features

While the previously described studies demonstrated accurate characterization of features associated with TCFAs, OCT is capable of identifying additional plaque components that may be associated with acute coronary events. These features are described below.

4.3.1 Calcific Nodules—Calcific nodules have been associated with plaque thrombosis in a minority of cases.[3,5] Calcium by OCT appears as a signal-poor region with a sharp delineation between the nodule and the surrounding tissue [Fig. 2(C)]. In our histopathologic study of plaque characterization, we were able to use this criterion to diagnose calcific nodules with 96% sensitivity and 97% specificity.[55]

4.3.2 Thrombus—Differentiation of thrombus from plaque is critical for accurate plaque characterization. In addition, there is evidence to suggest that thrombus type, platelet-rich versus red-blood-cell-rich, is an indicator of the flow conditions associated with the thrombus formation and could be an important predictor of the efficacy of thrombolytic therapy.[67,68] We have conducted a study to correlate histopathologic sections of thrombus with OCT. Our preliminary results suggest that a "red" thrombus (red-blood-cell-rich) rapidly attenuates the signal in a manner similar to whole blood [Fig. 4(A)]. In contrast, a "white" thrombus (platelet-rich) appears to exhibit a homogeneous moderate-strong signal with significantly less attenuation [Fig. 4(B)].[60] In our experience, both forms of thrombus are usually easily distinguished from the arterial wall proper.

4.3.3 Macrophages at the Cap-Lipid Pool Border—High-resolution cross-sectional optical imaging affords the unique opportunity to study the location of macrophage accumulations within a given plaque cross-section. Using our macrophage data set,[66] we found that 84% of OCT images demonstrated a high signal at the junction between the cap and the lipid pool [Fig. 5(A) and 5(B)] when CD68 staining at this interface was greater than 50%.

4.3.4 Giant Cells—Multinucleated macrophages, or giant cells, are an inflammatory response to a foreign body (e.g., cholesterol crystals) within atherosclerotic plaques. Giant cells can be visualized by OCT as large highly reflecting regions within the cap and at the cap-lipid pool interface [Fig. 5(C) and 5(D)].

4.3.5 Cholesterol Crystals—Research investigating the biomechanical properties of atherosclerotic plaques has shown that the presence of cholesterol crystals increases the stiffness of lipid pools, and as a result, may decrease the likelihood of plaque rupture.[69] Images of cholesterol crystals demonstrate oriented, linear, highly reflecting structures within the plaques [Fig. 5(E) and 5(F)].[70]

5 Clinical Studies

Histopathologic validation of qualitative and quantitative image criteria ex vivo provided a foundation for interpreting data obtained from living human patients. Between January 2000 and September 2003, a total of 86 patients undergoing routine percutaneous transluminal coronary intervention (PTCI) were enrolled in a study at the Massachusetts General Hospital (Boston, MA) to investigate the feasibility of intracoronary OCT. Informed consent was obtained for all patients. Imaging was performed in culprit lesions and remote sites with IVUS and OCT pre- and post-coronary intervention.[60,71] Clear visualization of the arterial wall was accomplished by use of intermittent saline flushes (8–10 cc) through the guide catheter. All

NIH-PA Author Manuscript

NIH-PA Author Manuscript

NIH-PA Author Manuscript

patients tolerated the procedure well without complications. Images demonstrating detailed arterial microstructure were successfully obtained in all patients studied and in all three major coronary arteries.[60,71] To compare IVUS and OCT, images were registered by angiographic visualization of the catheter tip, anatomical landmarks, and guide catheter tip location. Summaries of the results from our clinical study are described below:

OCT images obtained in living patients contained the same image features as those obtained ex vivo

All of the characteristics of macrophage-rich TCFAs as well as the additional plaque features described in the previous section were observed in vivo; there were no image features in the clinical data that had not been observed ex vivo (Fig. 6).[60] These observations suggest that image interpretation criteria and algorithms validated ex vivo can also be applied to images obtained from patients.

OCT observations were consistent with IVUS, the current gold standard for intracoronary imaging.[60]

Although IVUS is unable to resolve microstructural features associated with vulnerable plaque, it can identify nonatherosclerotic (normal) vessels, large thrombi, calcific deposits, and pronounced arterial disruptions. While unconfirmed, indirect evidence suggests that IVUS may detect large lipid deposits.[24] A study was conducted, comparing 17 OCT-IVUS image pairs obtained from 10 patients.[60] In all cases where IVUS identified these characteristics, blinded OCT observations were consistent (Table 1). OCT detected additional cases of intimal hyperplasia, thrombus, intimal disruption, and lipid pool not identified by IVUS.[60]

Imaging of culprit lesions demonstrated a higher prevalence of TCFA in patients with acute coronary disease than patients with stable coronary disease.[72]

In this analysis, TCFA was defined as a plaque with lipid area ≥2 quadrants and cap thickness <65 μm. A summary of the OCT findings, obtained from 57 patients with varying clinical presentations of coronary artery disease, is depicted in Table 2.[72] From these 57 patients, 20 presented with AMI, 20 with an acute coronary syndrome (ACS), and 17 with stable angina pectoris (SAP).[73] TCFAs identified by OCT were found in 13 AMI patients (65%), 9 with ACS (45%), and 3 with SAP (18%).[72] TCFAs were more prevalent in acute presentations (AMI and ACS) of CAD (55% versus 18%, p=0.012).[72] Plaque disruption was found more frequently in acute CAD (20% versus 12%, p=0.053) and calcifications were more frequent in stable disease (41% versus 12%, p=0.049).[72] These findings represent the first observation of presentation-dependent plaque morphology in living human patients and confirm our current knowledge of the relationship between morphology and patient outcome that has been obtained in previous autopsy studies.[3–7]

Macrophage content was significantly higher in fibroatheroma caps in patients with acute presentations of CAD, versus caps in patients with SAP.[74,75]

For this study, we created NSD (macrophage density) images (Fig. 7) and analyzed the macrophage distributions in both culprit and remote plaques (n=225) of 49 patients with different clinical syndromes. Macrophage density was found to be significantly higher in the AMI (5.54±1.48%) and ACS (5.86±2.01%) groups compared to the SAP group (4.14±1.81%) (p<0.003).[74,75]

Both focal and multi-focal elevations of macrophage density were associated with severity of clinical presentation.[75]

There is great interest in understanding the role of focal versus multi-focal plaque features in the pathogenesis of acute coronary thrombosis. The unique ability of OCT to quantify

NIH-PA Author Manuscript

NIH-PA Author Manuscript

NIH-PA Author Manuscript

macrophage content and observe the spatial distribution of plaque macrophages provides a valuable tool for investigating this critical question. Supporting the concept of focal risk, sites of plaque rupture demonstrated a greater macrophage density than nonrupture sites (6.95 ±0.48%, 5.71±0.37%; p=0.01).[75] In addition, macrophage density was significantly higher at the surface (first 50 μm) of culprit plaques in comparison to remote lesions, indicating that superficial macrophages confer a higher risk for developing an acute thrombus.[75] This finding represents a new understanding of the role of macrophages in the pathogenesis of acute coronary disease and may provide an additional parameter to assess individual plaque risk.

We also found evidence in support of the multi-focal hypothesis. Macrophage densities at remote sites were correlated with measurements at culprit sites within the same patient (r=0.66; p=0.01).[75] Fibrous plaques, which are not considered to be high-risk lesions, had a higher macrophage content in patients with acute disease, compared with stable patients (p=0.025).[75] Taken together, these results suggest that both focal and multi-focal macrophage distributions play important roles governing the severity of CAD.

6 Current Technology Challenges

Studies conducted with OCT clearly demonstrate the potential of this technology for impacting the management of CAD. However, limitations of current technology may preclude widespread use. Most importantly, due to its scattering and absorption, removal of blood interposed between the catheter and the arterial wall is required in order to obtain a clear, unobstructed view. Saline purging adequately removes blood from the field, but at current imaging frame rates (4–8 frames/ s), intracoronary OCT with saline flushing reduces to a single cross-sectional measurement. As a result, large area screening of vessel pathology required for widespread adoption is untenable with this paradigm. Balloon occlusion with saline purging, such as is commonly employed during angioscopy, remains a viable option for certain interventional communities.[42,76] However, this technique is not favored in the United States. Strategies such as reducing the scattering of blood by administering an index matching fluid or administration of a transparent oxygen-carrying blood substitute have been proposed to reduce the blood-attenuation problem.[77,78] More research needs to be conducted in these areas to determine the clinical viability of these methods. Another line of attack for overcoming the blood-attenuation problem is to increase the frame rate significantly, which can commensurately increase the information yield per purge. While conventional time-domain OCT systems have a frame rate of approximately 4–8 frames/ s, new frequency-domain OCT technology, spectral-domain OCT (SD-OCT)[79–83] and optical frequency domain imaging (OFDI), enable more than an order of magnitude higher frame rates.[84–86] Due to their high speeds, these second-generation OCT systems further open up the possibility of conducting three-dimensional comprehensive volumetric microscopy of long arterial segments.

One common misconception regarding OCT is that it can replace intravascular ultrasound. In fact, each technology excels at different tasks. IVUS obtains images through blood with approximately 100-μm resolution and a depth of penetration of approximately 1.0 cm. OCT on the other hand obtains images with much higher resolution, but cannot penetrate as deeply (~2 mm). As a result, OCT is particularly well suited to investigating microscopic features at the surface of the arterial wall, which are characteristic of high-risk vulnerable plaques. However, the infrared light utilized by OCT does not reach the back wall of thick atherosclerotic lesions and therefore this technology is probably not appropriate for evaluating pathology such as remodeling that is manifested by alterations of the elastic laminae.

Separate from the depth of penetration issue, conventional time-domain technology also has a limited depth range over which signals can be obtained. This limited ranging depth presents difficulties visualizing the entire arterial circumference, notably when the catheter is

NIH-PA Author Manuscript

NIH-PA Author Manuscript

NIH-PA Author Manuscript

eccentrically placed within a large diameter vessel. Auto-ranging, which adaptively adjusts the RSOD galvanometer to follow the lumen of the arterial wall, is one viable solution to this problem.[87] Additionally, second generation OFDI systems[84] inherently provide up to 7.0 mm of ranging depth, which is sufficient to visualize the entire artery even at the coronary ostia.

7 Conclusion

To date, optical coherence tomography has had a tangible impact on the quest to understand and identify the vulnerable plaque. It is the only method demonstrated to be capable of measuring all of the microscopic features associated with TCFAs. Our knowledge of the morphology of plaques associated with AMI, previously predicated on retrospective autopsy studies, has now been confirmed in living human patients with this technology. New information regarding macrophage distributions in patients with severe CAD, and insight into the focal and diffuse nature of the inflammatory atherosclerotic process has been uncovered.

The promise of intracoronary OCT is great, yet important challenges still remain. Much needs to be learned about the disease in order to ascertain the eventual role of this or any other intravascular modality in clinical practice. The prevalence, incidence, and natural history of high-risk lesions are presently poorly understood. Studies are currently underway using OCT and other imaging modalities to investigate the evolution of individual coronary lesions. Tests capable of screening a large population to determine patients that require more detailed intracoronary evaluation must be developed. Local treatment strategies have been proposed, including lesion stabilization with drug-eluting stents[88,89] and photodynamic therapy,[90,91] but the long-term clinical viability of these approaches is currently unknown. While there is still much to be done, we anticipate that the unique capabilities of OCT as an investigational tool for high-risk lesions will serve the cardiology community well as it advances to understand, identify, and ultimately treat the vulnerable plaque.

Acknowledgments

Studies by the authors described in this manuscript were funded in part by the Center for Integration of Medicine and Innovative Technology (development of the imaging platform), Guidant Corporation, and the National Institutes of Health (grants R01-HL70039 and R01-HL76398). We gratefully acknowledge Masamichi Takano for his assistance with OCT imaging of thrombus.

References

1. American Heart Association. Heart and Stroke Facts: Statistical Supplement. 1996.
2. American Heart Association. Heart Disease and Stroke Statistics—2003 Update. 2003.
3. Kolodgie FD, Burke AP, Farb A, Gold HK, Yuan J, Narula J, Finn AV, Virmani R. The thin-cap fibroatheroma: a type of vulnerable plaque: the major precursor lesion to acute coronary syndromes. Curr. Opin. Cardiol 2001;16:285–292. [PubMed: 11584167]
4. Virmani R, Kolodgie FD, Burke AP, Farb A, Schwartz SM. Lesions from sudden coronary death: a comprehensive morphological classification scheme for atherosclerotic lesions. Arterioscler., Thromb., Vasc. Biol 2000;20:1262–1275. [PubMed: 10807742]
5. Virmani R, Burke AP, Farb A, Kolodgie FD. Pathology of the unstable plaque. Prog. Cardiovasc. Dis 2002;44:349–356. [PubMed: 12024333]
6. Davies MJ. Stability and instability: two faces of coronary atherosclerosis. The Paul Dudley White Lecture 1995. Circulation 1996;94:2013–2020. [PubMed: 8873680]
7. Falk E. Why do plaques rupture? Circulation 1992;86:III30–III42. [PubMed: 1424049]
8. Davies MJ. Detecting vulnerable coronary plaques. Lancet 1996;347:1422–1423. [PubMed: 8676621]
9. Sukhova GK, Schonbeck U, Rabkin E, Schoen FJ, Poole AR, Billinghurst RC, Libby P. Evidence for increased collagenolysis by interstitial collagenases-1 and -3 in vulnerable human atheromatous plaques. Circulation 1999;99:2503–2509. [PubMed: 10330380]

NIH-PA Author Manuscript

NIH-PA Author Manuscript

NIH-PA Author Manuscript

10. Cheng GC, Loree HM, Kamm RD, Fishbein MC, Lee RT. Distribution of circumferential stress in ruptured and stable atherosclerotic lesions. A structural analysis with histopathological correlation. Circulation 1993;87:1179–1187. [PubMed: 8462145]
11. Lee RT, Grodzinsky AJ, Frank EH, Kamm RD, Schoen FJ. Structure-dependent dynamic mechanical behavior of fibrous caps from human atherosclerotic plaques. Circulation 1991;83:1764–1770. [PubMed: 2022029]
12. Moreno PR, Bernardi VH, Lopez-Cuellar J, Murcia AM, Palacios IF, Gold HK, Mehran R, Sharma SK, Nemerson Y, Fuster V, Fallon JT. Macrophages, smooth muscle cells, and tissue factor in unstable angina. Implications for cell-mediated thrombogenicity in acute coronary syndromes. Circulation 1996;94:3090–3097. [PubMed: 8989114]
13. Zaman AG, Helft G, Worthley SG, Badimon JJ. The role of plaque rupture and thrombosis in coronary artery disease. Atherosclerosis 2000;149:251–266. [PubMed: 10729375]
14. van der Wal AC, Becker AE, van der Loos CM, Das PK. Site of intimal rupture or erosion of thrombosed coronary atherosclerotic plaques is characterized by an inflammatory process irrespective of the dominant plaque morphology. Circulation 1994;89:36–44. [PubMed: 8281670]
15. Farb A, Burke AP, Tang AL, Liang TY, Mannan P, Smialek J, Virmani R. Coronary plaque erosion without rupture into a lipid core. A frequent cause of coronary thrombosis in sudden coronary death. Circulation 1996;93:1354–1363. [PubMed: 8641024]
16. Arbustini E, Grasso M, Diegoli M, Pucci A, Bramerio M, Ardissino D, Angoli L, de Servi S, Bramucci E, Mussini A, et al. Coronary atherosclerotic plaques with and without thrombus in ischemic heart syndromes: a morphologic, immunohistochemical, and biochemical study. Am. J. Cardiol 1991;68:36B–50B.
17. Rioufol G, Finet G, Ginon I, Andre-Fouet X, Rossi R, Vialle E, Desjoyaux E, Convert G, Huret JF, Tabib A. Multiple atherosclerotic plaque rupture in acute coronary syndrome: a three-vessel intravascular ultrasound study. Circulation 2002;106:804–808. [PubMed: 12176951]
18. Biasucci LM, Liuzzo G, Colizzi C, Maseri A. The role of cytokines in unstable angina. Expert Opin. Investig. Drugs 1998;7:1667–1672.
19. Cascells W, Naghavi M, Willerson JT. Vulnerable atherosclerotic plaque: a multfocal disease. Circulation 2003;107:2072–2075. [PubMed: 12719287]
20. Krams R, Segers D, Gourabi BM, Maat W, Cheng C, van Pelt C, van Damme LC, de Feyter P, van der Steen T, de Korte CL, Serruys PW. Inflammation and atherosclerosis: mechanisms underlying vulnerable plaque. J. Intery. Cardiol 2003;16:107–113.
21. Maseri A, Fuster V. Is there a vulnerable plaque? Circulation 2003;107:2068–2071. [PubMed: 12719286]
22. Kereiakes DJ. The emperor's clothes: in search of the vulnerable plaque. Circulation 2003;107:2076–2077. [PubMed: 12719288]
23. Yock PG, Fitzgerald PJ. Intravascular ultrasound: state of the art and future directions. Am. J. Cardiol 1998;81:27E–32E. [PubMed: 9462601]
24. Yamaguchi M, Terashima M, Awano K, Kijima M, Nakatani S, Daikoku S, Ito K, Yasamura Y, Miyatake K. Morphology of vulnerable coronary plaques: insights from follow-up of patients examined by intravascular ultrasound before an acute coronary event. J. Am. Coll. Cardiol 2000;35:106–111. [PubMed: 10636267]
25. Martin AJ, Ryan LK, Gotlieb AI, Henkelman RM, Foster FS. Arterial imaging: comparison of high-resolution US and MR imaging with histologic correlation. Radiographics 1997;17:189–202. [PubMed: 9017808]
26. Schoenhagen P, Nissen SE. Understanding coronary artery disease: tomographic imaging with intravascular ultrasound. Heart 2002;88:91–96. [PubMed: 12067962]
27. Tobis JM, Mallery J, Mahon D, Lehmann K, Zalesky P, Griffith J, Gessert J, Moriuchi M, McRae M, Dwyer M-L, Greep N, Henry WL. Intravascular ultrasound imaging of human cornary arteries in vivo: analysis of tissue characterizations with comparison to in vitro histological specimens. Circulation 1991;83:913–926. [PubMed: 1999040]
28. Prati F, Arbustini E, Labellarte A, Dal Bello B, Sommariva L, Mallus MT, Pagano A, Boccanelli A. Correlation between high frequency intravascular ultrasound and histomorphology in human coronary arteries. Heart 2001;85:567–570. [PubMed: 11303012]

NIH-PA Author Manuscript

NIH-PA Author Manuscript

NIH-PA Author Manuscript

29. Rumberger JA, Behrenbeck T, Breen JF, Sheedy PF II. Coronary calcification by electron beam computed tomography and obstructive coronary artery disease: a model for costs and effectiveness of diagnosis as compared with conventional cardiac testing methods. J. Am. Coll. Cardiol 1999;33:453–462. [PubMed: 9973026]
30. Wong ND, Vo A, Abrahamson D, Tobis JM, Eisenberg H, Detrano RC. Detection of coronary artery calcium by ultrafast computed tomography and its relation to clinical evidence or coronary artery disease. Am. J. Cardiol 1994;73:223–227. [PubMed: 8296750]
31. Budoff MJ, Brundage BH. Electron beam computed tomography: screening for coronary artery disease. Clin. Cardiol 1999;22:554–558. [PubMed: 10486694]
32. Naghavi M, Madjid M, Khan MR, Mohammadi RM, Willerson JT, Casscells SW. New developments in the detection of vulnerable plaque. Current Atherosclerosis Rep 2001;3:125–135.
33. Baer FM, Theissen P, Crnac J, Schmidt M, Jochims M, Schicha H. MRI assessment of coronary artery disease. Rays 1999;24:46–59. [PubMed: 10358383]
34. Toussaint JF, LaMuraglia GM, Southern JF, Fuster V, Kantor HL. Magnetic resonance images lipid, fibrous, calcified, hemorrhagic, and thrombotic components of human atherosclerosis in vivo. Circulation 1996;94:932–938. [PubMed: 8790028]
35. Helft G, Worthley SG, Fuster V, Fayad ZA, Zaman AG, Corti R, Fallon JT, Badimon JJ. Progression and regression of atherosclerotic lesions: monitoring with serial noninvasive magnetic resonance imaging. Circulation 2002;105:993–998. [PubMed: 11864931]
36. Machado JC, Foster FS. Ultrasonic integrated backscatter coefficient profiling of human coronary arteries in vitro. IEEE Trans. Ultrason. Ferroelectr. Freq. Control 2001;48:17–27. [PubMed: 11367784]
37. Urbani MP, Picano E, Parenti G, Mazzarisi A, Fiori L, Paterni M, Pelosi G, Landini L. In vivo radiofrequency-based ultrasonic tissue characterization of the atherosclerotic plaque. Stroke 1993;24:1507–1512. [PubMed: 8378954]
38. de Korte CL, van der Steen AFW, Cespedes EI, Pasterkamp G, Carlier SG, Mastik F, Schoneveld AH, Serruys PW, Bom N. Characterization of plaque components and vulnerability with intravascular ultrasound elastography. Phys. Med. Biol 2000;45:1465–1475. [PubMed: 10870704]
39. Ueda Y, Asakura M, Yamaguchi O, Hirayama A, Hori M, Kodama K. The healing process of infarct-related plaques. J. Am. Coll. Cardiol 2001;38:1916–1922. [PubMed: 11738294]
40. Asakura M, Ueda Y, Yamaguchi O, Adachi T, Hirayama A, Hori M, Kodama K. Extensive development of vulnerable plaques as a pan-coronary process in patients with myocardial infarction: an angioscopic study. J. Am. Coll. Cardiol 2001;37:1284–1288. [PubMed: 11300436]
41. Kodama K, Hirayama A, Ueda Y. Usefulness of coronary angioscopy for the evaluation of hyperlipidemia. Nippon Rinsho 2002;60:927–932. [PubMed: 12029995]
42. Mizuno K, Nakamura H. Percutaneous coronary angioscopy: present role and future direction. Ann. Med 1993;25:1–2. [PubMed: 8435180]
43. Waxman S. Characterization of the unstable lesion by angiography, angioscopy, and intravascular ultrasound. Cardiol. Clin 1999;17:295–305. [PubMed: 10384828]viii
44. Moreno PR, Lodder RA, Purushothaman KR, Charash WE, O'onnor WN, Muller JE. Detection of lipid pool, thin fibrous cap, and inflammatory cells in human aortic atherosclerotic plaques by near-infrared spectroscopy. Circulation 2002;105:923–927. [PubMed: 11864919]
45. Christov A, Korol RM, Dai E, Liu L, Guan H, Bernards MA, Cavers PB, Susko D, Lucas A. In vivo optical analysis of quantitative changes in collagen and elastin during arterial remodeling. Photochem. Photobiol 2005;81:457–466. [PubMed: 15560737]
46. Marcu L, Fang Q, Jo JA, Papaioannou T, Dorafshar A, Reil T, Qiao JH, Baker JD, Freischlag JA, Fishbein MC. In vivo detection of macrophages in a rabbit atherosclerotic model by time-resolved laser-induced fluorescence spectroscopy. Atherosclerosis 2005;181:295–303. [PubMed: 16039283]
47. Marcu L, Fishbein MC, Maarek JM, Grundfest WS. Discrimination of human coronary artery atherosclerotic lipid-rich lesions by time-resolved laser-induced fluorescence spectroscopy. Arterioscler., Thromb., Vasc. Biol 2001;21:1244–1250. [PubMed: 11451759]
48. Romer TJ, Brennan JF III, Fitzmaurice M, Feldstein ML, Deinum G, Myles JL, Kramer JR, Lees RS, Feld MS. Histopathology of human coronary atherosclerosis by quantifying its chemical composition with Raman spectroscopy. Circulation 1998;97:878–885. [PubMed: 9521336]

NIH-PA Author Manuscript

NIH-PA Author Manuscript

NIH-PA Author Manuscript

49. Buschman HP, Deinum G, Motz JT, Fitzmaurice M, Kramer JR, van der Laarse A, Bruschke AV, Feld MS. Raman microspectroscopy of human coronary atherosclerosis: biochemical assessment of cellular and extracellular morphologic structures in situ. Cardiovasc. Pathol 2001;10:69–82. [PubMed: 11425600]
50. Casscells W, Hathorn B, David M, Krabach T, Vaughn WK, McAllister HA, Bearman G, Willerson JT. Thermal detection of cellular infiltrates in living atherosclerotic plaques: possible implications for plaque rupture and thrombosis. Lancet 1996;347:1447–1451. [PubMed: 8676628]
51. Stefanadis C, Toutouzas K, Tsiamis E, Stratos C, Vavuranakis M, Kallikazaros I, Panagiotakos D, Toutouzas P. Increased local temperature in human coronary atherosclerotic plaques: an independent predictor of clinical outcome in patients undergoing a percutaneous coronary intervention. J. Am. Coll. Cardiol 2001;37:1277–1283. [PubMed: 11300435]
52. van der Meer FJ, Faber DJ, Baraznji Sassoon DM, Aalders MC, Pasterkamp G, van Leeuwen TG. Localized measurement of optical attenuation coefficients of atherosclerotic plaque constituents by quantitative optical coherence tomography. IEEE Trans. Med. Imaging 2005;24:1369–1376. [PubMed: 16229422]
53. Patel NA, Stamper DL, Brezinski ME. Review of the ability of optical coherence tomography to characterize plaque, including a comparison with intravascular ultrasound. Cardiovasc. Intervent Radiol 2005;28:1–9. [PubMed: 15772720]
54. Regar E, Schaar JA, Mont E, Virmani R, Serruys PW. Optical coherence tomography. Cardiovasc. Radiat. Med 2003;4:198–204. [PubMed: 15321058]
55. Yabushita H, Bouma BE, Houser SL, Aretz HT, Jang IK, Schlendorf K, Kauffman CR, Shishkov M, Kang DH, Halpern EF, Tearney GJ. Characterization of human atherosclerosis by optical coherence tomography. Circulation 2002;106:1640–1645. [PubMed: 12270856]
56. Tearney GJ, Boppart SA, Bouma BE, Brezinski ME, Weissman NJ, Southern JF, Fujimoto JG. Scanning single-mode fiber optic catheter-endoscope for optical coherence tomography. Opt. Lett 1996;21:1–3. [PubMed: 19865284]
57. Brezinski ME, Tearney GJ, Bouma BE, Izatt JA, Hee MR, Swanson EA, Southern JF, Fujimoto JG. Optical coherence tomography for optical biopsy: properties and demonstration of vascular pathology. Circulation 1996;93:1206–1213. [PubMed: 8653843]
58. Tearney GJ, Brezinski ME, Bouma BE, Boppart SA, Pitris C, Southern JF, Fujimoto JG. In vivo endoscopic optical biopsy with optical coherence tomography. Science 1997;276:2037–2039. [PubMed: 9197265]
59. Bouma BE, Tearney GJ. Power-efficient nonreciprocal interferometer and linear-scanning fiber-optic catheter for optical coherence tomography. Opt. Lett 1999;24:531–533. [PubMed: 18071562]
60. Jang IK, Bouma BE, Kang DH, Park SJ, Park SW, Seung KB, Choi KB, Shishkov M, Schlendorf K, Pomerantsev E, Houser SL, Aretz HT, Tearney GJ. Visualization of coronary atherosclerotic plaques in patients using optical coherence tomography. J. Am. Coll. Cardiol 2002;39:604–609. [PubMed: 11849858]
61. Tearney GJ, Bouma BE, Fujimoto JG. High-speed phase- and group-delay scanning with a grating-based phase control delay line. Opt. Lett 1997;22:1811–1813. [PubMed: 18188374]
62. Shishkov, M.; Bouma, BE.; Jang, IK.; Aretz, HT.; Houser, SL.; Brady, TJ.; Schlendorf, K.; Tearney, GJ. Optical coherence tomography of porcine coronary arteries in vivo; presented at the Optical Society of America Biomedical Topical Meetings 2000; Miami, FL. (unpublished)
63. Moreno PR, Falk E, Palacios IF, Newell JB, Fuster V, Fallon JT. Macrophage infiltration in acute coronary syndromes: implications for plaque rupture. Circulation 1994;90:775–778. [PubMed: 8044947]
64. Lendon CL, Davies MJ, Born GV, Richardson PD. Atherosclerotic plaque caps are locally weakened when macrophage density is increased. Atherosclerosis 1991;87:87–90. [PubMed: 1872926]
65. Davies MJ, Richardson PD, Woolf N, Katz DR, Mann J. Risk of thrombosis in human atherosclerotic plaques: role of extracellular lipid, macrophage, and smooth muscle cell content. Br. Heart J 1993;69:377–381. [PubMed: 8518056]
66. Tearney GJ, Yabushita H, Houser SL, Aretz HT, Jang IK, Schlendorf K, Kauffman CR, Shishkov M, Halpern EF, Bouma BE. Quantification of macrophage content in atherosclerotic plaques by optical coherence tomography. Circulation 2003;107:113–119. [PubMed: 12515752]

NIH-PA Author Manuscript

NIH-PA Author Manuscript

NIH-PA Author Manuscript

67. Goto S, Handa S. Coronary thrombosis. Effects of blood flow on the mechanism of thrombus formation. Jpn. Heart J 1998;39:579–596. [PubMed: 9925990]
68. Jang IK, Hursting MJ. When heparins promote thrombosis: review of heparin-induced thrombocytopenia. Circulation 2005;111:2671–2683. [PubMed: 15911718]
69. Loree HM, Grodzinsky AJ, Park SY, Gibson LJ, Lee RT. Static circumferential tangential modulus of human atherosclerotic tissue. J. Biomech 1994;27:195–204. [PubMed: 8132688]
70. Tearney GJ, Jang IK, Bouma BE. Evidence of cholesterol crystals in atherosclerotic plaque by optical coherence tomographic (OCT) imaging. Eur. Heart J 2003;24:1462. [PubMed: 12909076]
71. Jang IK, Tearney G, Bouma B. Visualization of tissue prolapse between coronary stent struts by optical coherence tomography: comparison with intravascular ultrasound. Circulation 2001;104:2754. [PubMed: 11723031]
72. Jang IK, Tearney GJ, MacNeill B, Takano M, Moselewski F, Iftima N, Shishkov M, Houser S, Aretz HT, Halpern EF, Bouma BE. In vivo characterization of coronary atherosclerotic plaque by use of optical coherence tomography. Circulation 2005;111:1551–1555. [PubMed: 15781733]
73. Cannon CP, Battler A, Brindis RG, Cox JL, Ellis SG, Every NR, Flaherty JT, Harrington RA, Krumholz HM, Simoons ML, Van De Werf FJ, Weintraub WS, Mitchell KR, Morrisson SL, Brindis RG, Anderson HV, Cannom DS, Chitwood WR, Cigarroa JE, Collins-Nakai RL, Ellis SG, Gibbons RJ, Grover FL, Heidenreich PA, Khandheria BK, Knoebel SB, Krumholz HL, Malenka DJ, Mark DB, McKay CR, Passamani ER, Radford MJ, Riner RN, Schwartz JB, Shaw RE, Shemin RJ, Van Fossen DB, Verrier ED, Watkins MW, Phoubandith DR, Furnelli T. American College of Cardiology key data elements and definitions for measuring the clinical management and outcomes of patients with acute coronary syndromes. A report of the American College of Cardiology Task Force on Clinical Data Standards (Acute Coronary Syndromes Writing Committee). J. Am. Coll. Cardiol 2001;38:2114–2130. [PubMed: 11738323]
74. MacNeill BD, Bouma BE, Yabushita H, Jang IK, Tearney GJ. Intravascular optical coherence tomography: cellular imaging. J. Nucl. Cardiol 2005;12:460–465. [PubMed: 16084435]
75. MacNeill BD, Jang IK, Bouma BE, Iftimia N, Takano M, Yabushita H, Shishkov M, Kauffman CR, Houser SL, Aretz HT, DeJoseph D, Halpern EF, Tearney GJ. Focal and multi-focal plaque macrophage distributions in patients with acute and stable presentations of coronary artery disease. J. Am. Coll. Cardiol 2004;44:972–979. [PubMed: 15337206]
76. Uchida Y, Fumitaka N, Tomaru T, Morita T, Oshima T, Sasaki T, Morizuki S, Hirose J. Prediction of acute coronary syndromes by percutaneous coronary angioscopy in patients with stable angina. Am. Heart J 1995;130:195–203. [PubMed: 7631596]
77. Brezinski M, Saunders K, Jesser C, Li X, Fujimoto J. Index matching to improve optical coherence tomography imaging through blood. Circulation 2001;103:1999–2003. [PubMed: 11306530]
78. Villard JW, Feldman MD, Kim J, Milner TE, Freeman GL. Use of a blood substitute to determine instantaneous murine right ventricular thickening with optical coherence tomography. Circulation 2002;105:1843–1849. [PubMed: 11956129]
79. Wojtkowski M, Srinivasan V, Fujimoto JG, Ko T, Schuman JS, Kowalczyk A, Duker JS. Three-dimensional retinal imaging with high-speed ultrahigh-resolution optical coherence tomography. Ophthalmology 2005;112:1734–1746. [PubMed: 16140383]
80. Wojtkowski M, Leitgeb R, Kowalczyk A, Fercher AF. Fourier domain OCT imaging of the human eye in vivo. Proc. SPIE 2002;4619:230–236.
81. Hausler G, Lindner MW. Coherence Radar and Spectral Radar - new tools for dermatological diagnosis. J. Biomed. Opt 1998;3:21–31.
82. Nassif N, Cense B, Park BH, Yun SH, Chen TC, Bouma BE, Tearney GJ, de Boer JF. In vivo human retinal imaging by ultrahigh-speed spectral domain optical coherence tomography. Opt. Lett 2004;29:480–482. [PubMed: 15005199]
83. de Boer JF, Cense B, Park BH, Pierce MC, earney GJ, Bouma BE. Improved signal-to-noise ratio in spectral-domain compared with time-domain optical coherence tomography. Opt. Lett 2003;28:2067–2069. [PubMed: 14587817]
84. Yun SH, Tearney GJ, de Boer JF, Iftimia N, Bouma BE. High-speed optical frequency domain imaging. Opt. Express 2003;11:2953–2963. [PubMed: 19471415]

NIH-PA Author Manuscript

NIH-PA Author Manuscript

NIH-PA Author Manuscript

85. Yun SH, Tearney GJ, Bouma BE, Park BH, de Boer JF. High-speed spectral-domain optical coherence tomography at 1.3 μm wavelength. Opt. Express 2003;26:3598–3604. [PubMed: 19471496]

86. Choma MA, Hsu K, Izatt JA. Swept source optical coherence tomography using an all-fiber 1300-nm ring laser source. J. Biomed. Opt 2005;10:044009.

87. Iftima N, Bouma BE, de Boer JF, Park BH, Cense B, Tearney GJ. Adaptive ranging for optical coherence tomography. Opt. Express 2004;12:4025–4034. [PubMed: 19483942]

88. Valgimigli M, van Mieghem CA, Ong AT, Aoki J, Granillo GA, McFadden EP, Kappetein AP, de Feyter PJ, Smits PC, Regar E, Van der Giessen WJ, Sianos G, de Jaegere P, Van Domburg RT, Serruys PW. Short-and long-term clinical outcome after drug-eluting stent implantation for the percutaneous treatment of left main coronary artery disease: insights from the Rapamycin-Eluting and Taxus Stent Evaluated At Rotterdam Cardiology Hospital registries (RESEARCH and T-SEARCH). Circulation 2005;111:1383–1389. [PubMed: 15781749]

89. Chieffo A, Stankovic G, Bonizzoni E, Tsagalou E, Iakovou I, Montorfano M, Airoldi F, Michev I, Sangiorgi MG, Carlino M, Vitrella G, Colombo A. Early and mid-term results of drug-eluting stent implantation in unprotected left main. Circulation 2005;111:791–795. [PubMed: 15699254]

90. Demidova TN, Hamblin MR. Macrophage-targeted photodynamic therapy. Intl. J. Immunopathol. Pharmacol 2004;17:117–126.

91. Kereiakes DJ, Szyniszewski AM, Wahr D, Herrmann HC, Simon DI, Rogers C, Kramer P, Shear W, Yeung AC, Shunk KA. Phase I drug and light dose-escalation trial of motexafin lutetium and far red light activation (phototherapy) in subjects with coronary artery disease undergoing percutaneous coronary intervention and stent deployment: procedural and long-term results. Circulation 2003;108:1310–1315. [PubMed: 12939212]

NIH-PA Author Manuscript

NIH-PA Author Manuscript

NIH-PA Author Manuscript

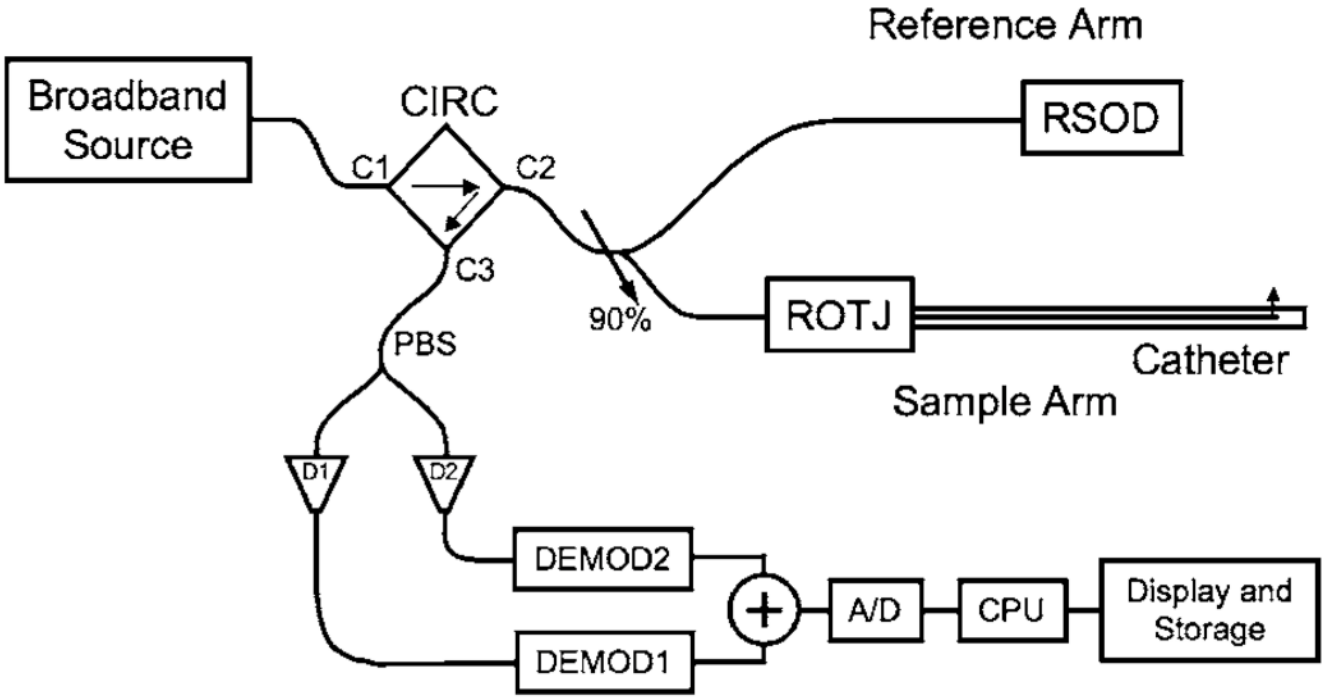

Fig. 1.

Schematic of the time-domain intracoronary optical coherence tomography system. Polarized, broad-bandwidth light passes through a circulator (CIRC, port C1 to port C2) and is split into reference and sample arms via a 10/90 fiber optic beam splitter. The optical path length (group delay) of the reference arm is scanned by translating the galvanometer of the rapidly scanning optical delay (RSOD) line. Sample arm light is coupled into the catheter by a rotating optical junction (ROTJ). Light returned from the reference and sample arms is combined at the splitter and transmitted back to the circulator at port C2. The circulator then passes this light through port C3 to a polarizing beam splitter (PBS). The two orthogonal polarization states are detected separately by photodiodes D1 and D2. The two signals are demodulated and summed to create the final output signal, which is digitized (A/D) and transferred to the CPU. Detection of the fringe patterns created by sample and reference arm interference allows one radial scan (A-line) to be constructed that maps tissue reflectivity axial or depth location. A cross-sectional image is generated by repeating this process at successive transverse locations on the sample while the ROTJ rotates the internal components of the catheter.

NIH-PA Author Manuscript
NIH-PA Author Manuscript
NIH-PA Author Manuscript

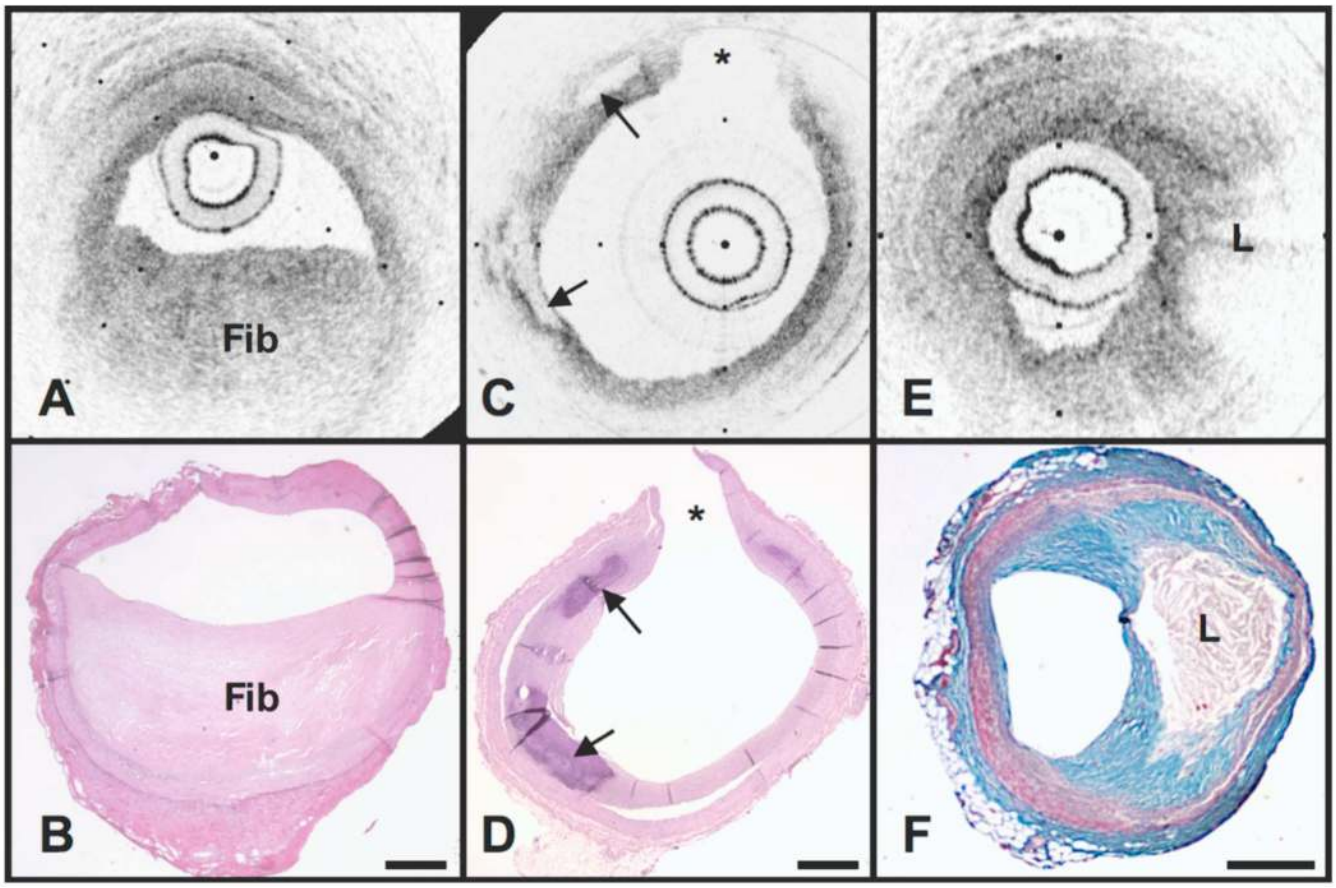

Fig. 2.

OCT images and corresponding histology for fibrous (A, B), calcific (C, D), and lipid-rich (E, F) plaque types (obtained ex vivo). In fibrous plaques, the OCT signal (Fib) is observed to be strong and homogeneous. In comparison, both calcific (arrows) and lipid-rich regions (L) appear as signal poor regions within the vessel wall. Lipid-rich plaques have diffuse or poorly demarcated borders while the borders of calcific nodules are sharply delineated. (B, D) Hematoxylin & Eosin; (F) Masson's trichome; original magnification 40×. Scale bars, tick marks, 500 μm.

NIH-PA Author Manuscript
NIH-PA Author Manuscript
NIH-PA Author Manuscript

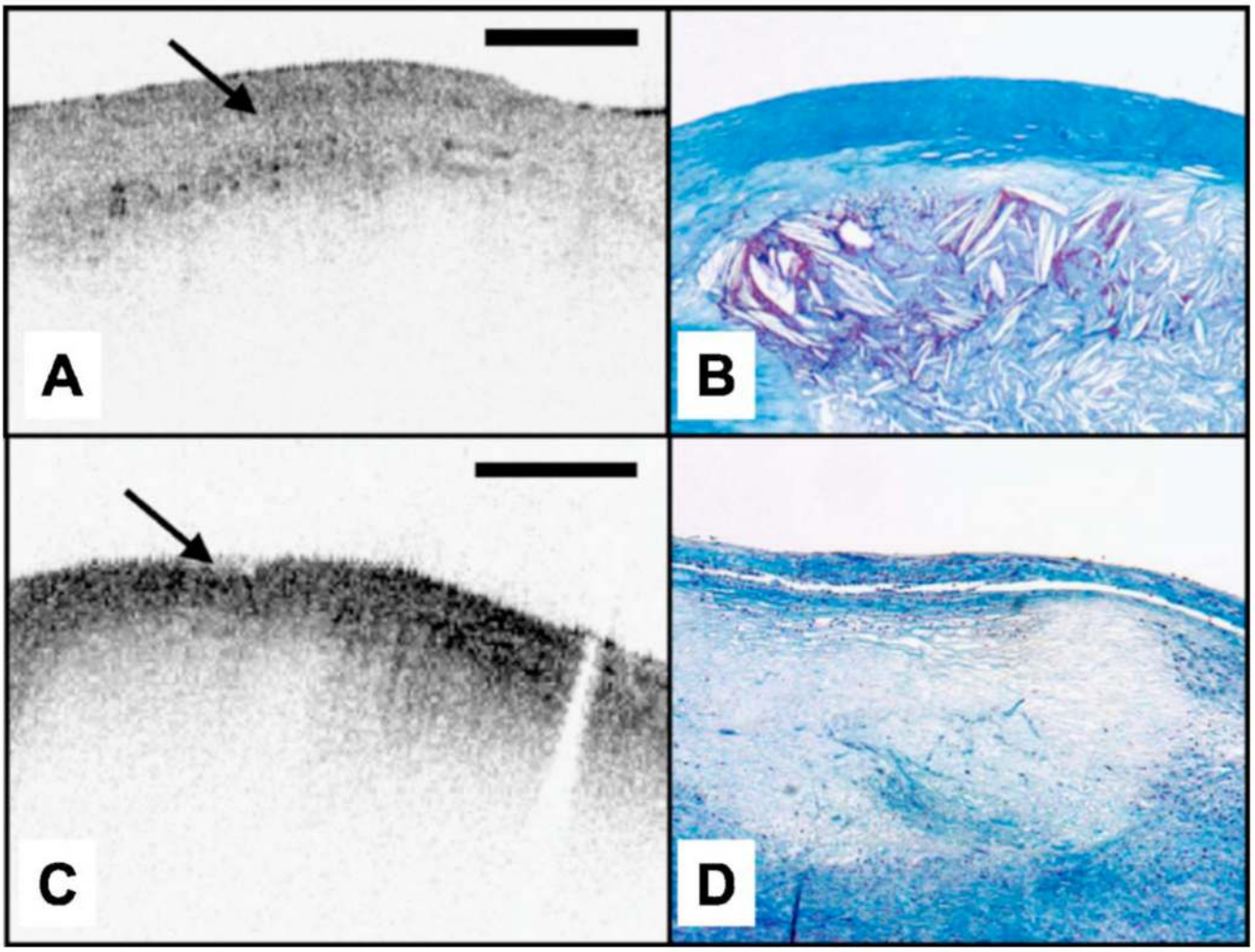

Fig. 3.
Images of atherosclerotic plaques (obtained ex vivo) (A) OCT image of a fibroatheroma with a low density of macrophages within the fibrous cap (arrow). (C) OCT image of a fibroatheroma with a high density of macrophages within the fibrous cap (arrow). (B, D) Histology corresponding to (A) and (C), respectively; Masson's trichome; original magnification 40×. Scale bars (both OCT and histology), 500 μm.

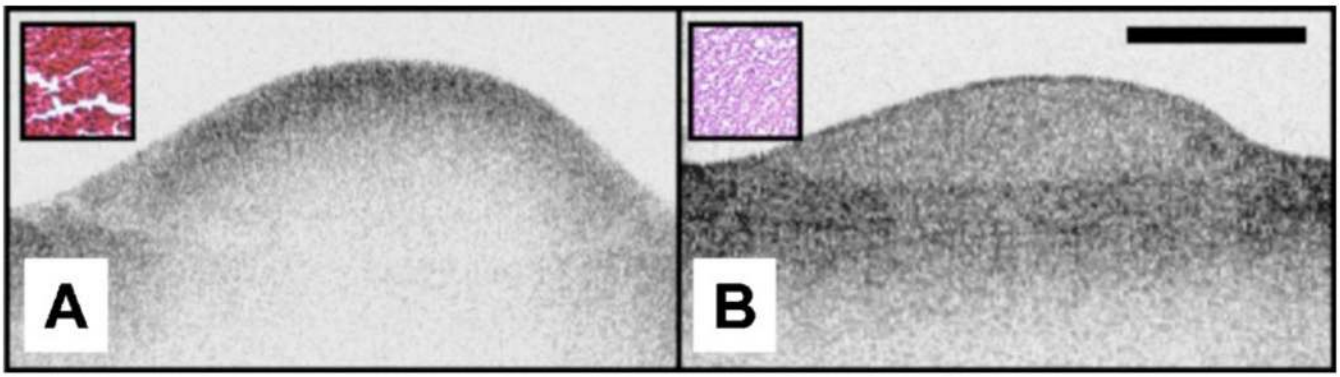

Fig. 4.
OCT images of red blood cell-rich (A) and platelet-rich (B) thrombi (obtained ex vivo). The red blood cell-rich thrombus demonstrates high OCT signal attenuation, whereas the platelet rich thrombus shows a homogeneous scattering signal with relatively little attenuation. Insets depict corresponding histology sections from each thrombus; Hematoxylin & Eosin; original magnification 40×. Scale bar, 500 μm.

NIH-PA Author Manuscript
NIH-PA Author Manuscript
NIH-PA Author Manuscript

NIH-PA Author Manuscript

NIH-PA Author Manuscript

NIH-PA Author Manuscript

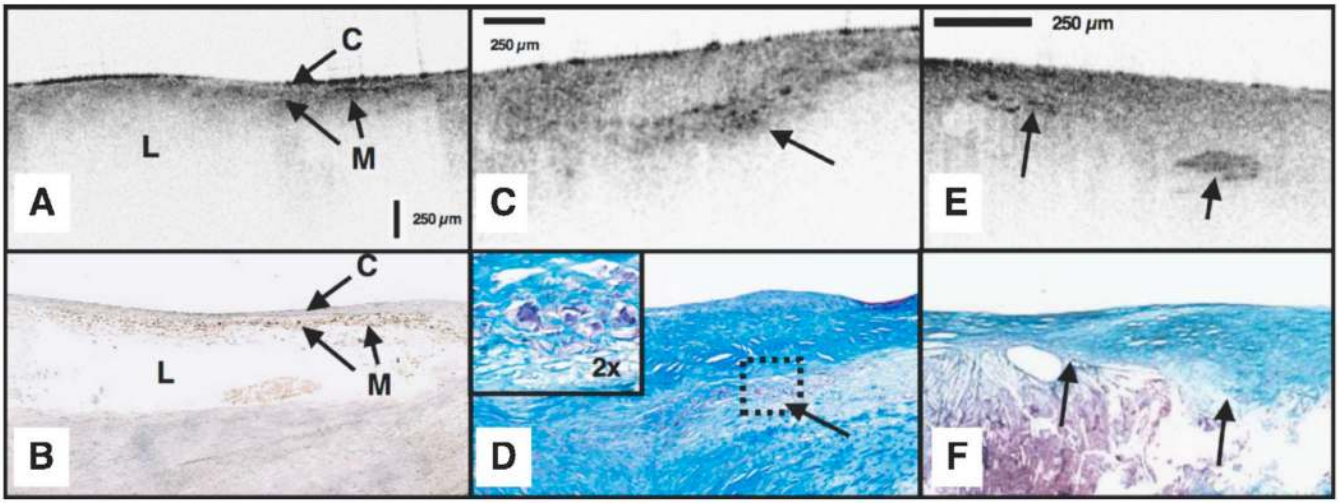

Fig. 5.

Images of atherosclerotic plaques (obtained ex vivo) (A) OCT image of a fibroatheroma with macrophages (M) present at the cap (C) lipid-pool (L) interface. (C) OCT image demonstrating giant cells (arrow). (E) Cholesterol crystals (arrows) appear as signal-rich linear structures. (B, D, and F) Histology corresponding to (A), (C), and (E); (B) CD68; (D, F) Masson's trichrome; original magnification 40×. Scale bars (both OCT and histology), 250 μm.

NIH-PA Author Manuscript

NIH-PA Author Manuscript

NIH-PA Author Manuscript

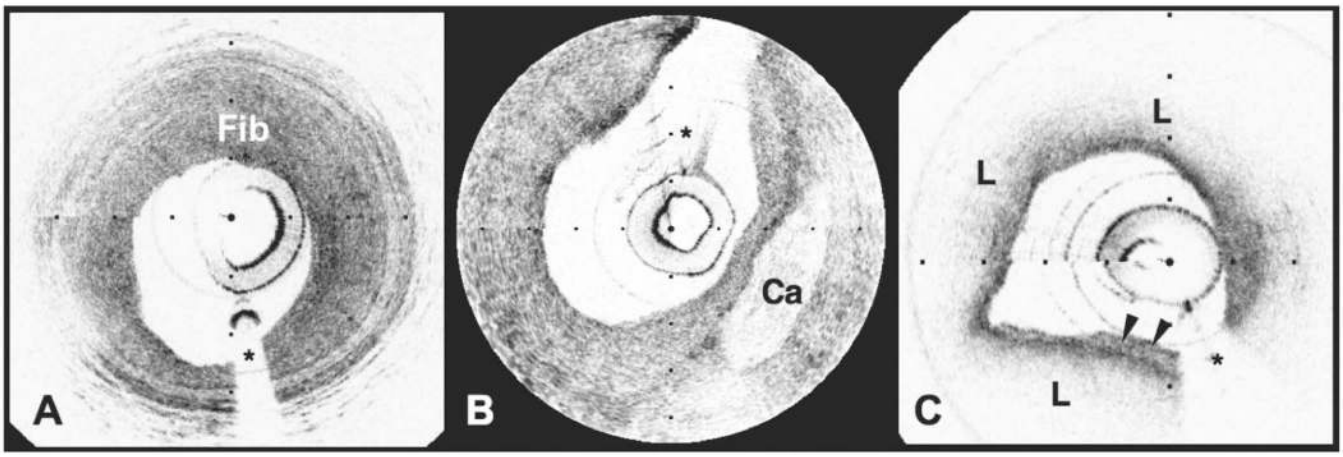

Fig. 6.

OCT images of coronary plaques acquired from living human patients (obtained in vivo). (A) Fibrous plaque (Fib); (B) calcific nodule (Ca); (C) TCFA with circumferential lipid pool (L) and a region consistent with a platelet-rich thrombus (arrowheads). The * represents guidewire artifacts. Tick marks, 500 μm.

NIH-PA Author Manuscript
NIH-PA Author Manuscript
NIH-PA Author Manuscript

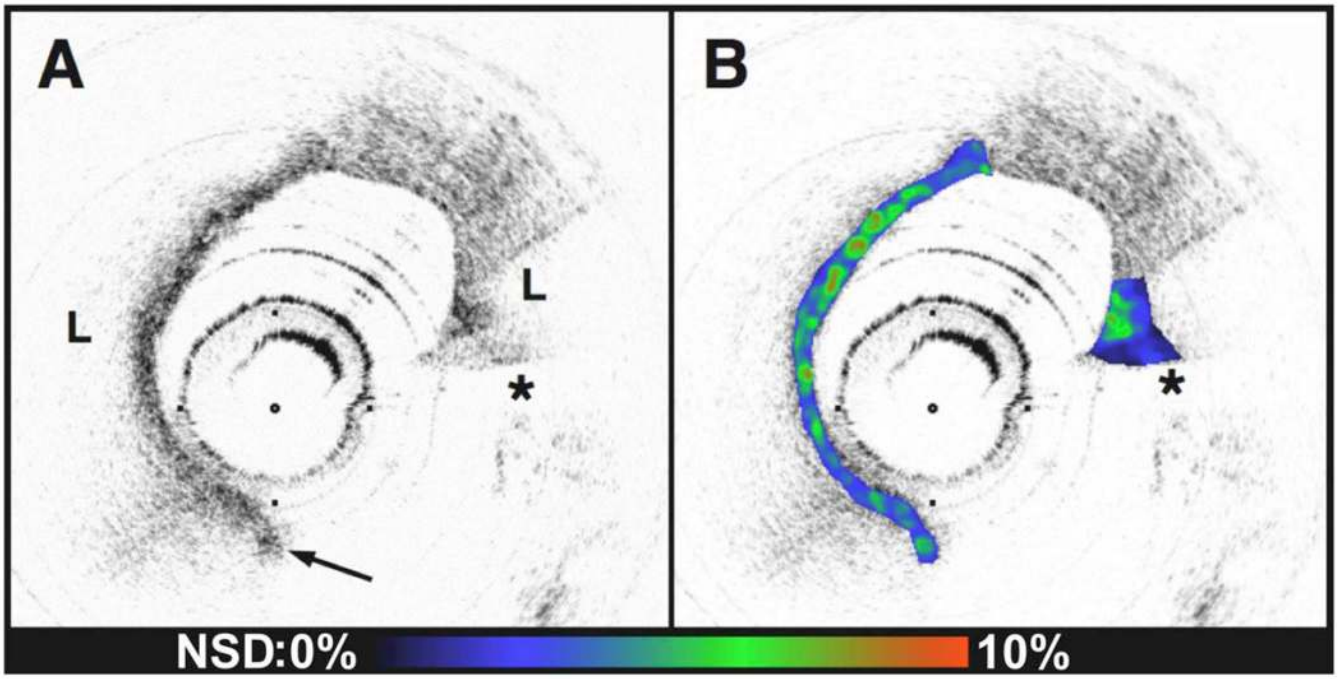

Fig. 7.

Conventional OCT image of a ruptured TCFA obtained from a patient with AMI (obtained in vivo). (B) In this image, macrophage density data (NSD) from the fibrous cap is displayed using a color look-up table. L, lipid pool; arrow, intimal disruption; *, guidewire artifacts. Tick marks, 500 μm.

NIH-PA Author Manuscript

NIH-PA Author Manuscript

NIH-PA Author Manuscript

Table 1

IVUS and OCT findings for corresponding image pairs (n=17). All features of the vessel wall structure identified by the IVUS reader were seen in the corresponding OCT image (column A). Additional findings by OCT that were not identified by the IVUS reader are enumerated in column B. (Taken from Ref. 60.)

Feature	(A) Identified by Both OCT and IVUS	(B) Identified by OCT Alone
Intimal hyperplasia	3 (3 patients)	8 (7 patients)
Internal elastic lamina	not evaluated	11 (8 patients)
External elastic lamina	not evaluated	10 (7 patients)
Plaque	17 (10 patients)	0
Fibrous plaque	13 (10 patients)	0
Calcific plaque	4 (4 patients)	0
Echolucent region	2 (2 patients)	2 (2 patients)

NIH-PA Author Manuscript

NIH-PA Author Manuscript

NIH-PA Author Manuscript

Table 2

OCT findings from MGH clinical study (*n*=57). TCFA indicates thin-cap fibroatheroma (lipid ≥2 quadrants +fibrous cap thickness ≤65 μm). (Taken from Ref. 72.)

Finding	AMI (*n*=20)	ACS (*n*=20)	SAP (*n*=17)	P
Lipid Plaque, No. of quadrants	18	18	15	
1	0	3	5	
2	7	8	5	
3	5	5	3	
4	6	2	2	
Lipid-rich plaque (≥2 quadrants)	18	15	10	0.09
Fibrous cap thickness (μm) (median)	47.0 (*n*=18)	53.8 (*n*=18)	102.6 (*n*=15)	0.034
TCFA	13 (*n*=18)	9 (*n*=18)	3 (*n*=15)	0.012
Plaque disruption	5	3	2	0.053
Calcification	2	3	7	0.049
Thrombus	4	5	6	